

The Holdout Randomization Test: Principled and Easy Black Box Feature Selection

Wesley Tansey^{*1,2}, Victor Veitch³, Haoran Zhang⁴, Raul Rabadan², and David M. Blei^{1,3,5}

¹Data Science Institute, Columbia University, New York, NY, USA

²Department of Systems Biology, Columbia University Medical Center, New York, NY, USA

³Department of Statistics, Columbia University, New York, NY, USA

⁴Department of Applied Mathematics and Applied Physics, Columbia University, New York, NY, USA

⁵Department of Computer Science, Columbia University, New York, NY, USA

Abstract

We consider the problem of feature selection using black box predictive models. For example, high-throughput devices in science are routinely used to gather thousands of features for each sample in an experiment. The scientist must then sift through the many candidate features to find explanatory signals in the data, such as which genes are associated with sensitivity to a prospective therapy. Often, predictive models are used for this task: the model is fit, error on held out data is measured, and strong performing models are assumed to have discovered some fundamental properties of the system. A model-specific heuristic is then used to inspect the model parameters and rank important features, with top features reported as “discoveries.” However, such heuristics provide no statistical guarantees and can produce unreliable results. We propose the holdout randomization test (HRT) as a principled approach to feature selection using black box predictive models. The HRT is similar to a permutation test, where each random reshuffling is a draw from the complete conditional distribution of the feature being tested. The HRT is model agnostic and produces a valid p -value for each feature, enabling control over the false discovery rate (or Type I error) for any predictive model. Further, the HRT is computationally efficient and, in simulations, has greater power than a competing knockoffs-based approach. Code is available at <https://github.com/tansey/hrt>.

1 Introduction

We consider the task of selecting the subset of features (X) that are relevant to an outcome (Y). Formally, the inferential goal is to conduct a conditional independence test for each feature X_j , with the null hypothesis:

$$H_0: X_j \perp\!\!\!\perp Y | X_{\cdot, -j}, \quad (1)$$

^{*}wt2274@cumc.columbia.edu (corresponding author)

where $X_{\cdot,-j}$ is every column in the feature matrix X except $X_{\cdot j}$. Under H_0 , the feature contains no additional information about Y that is not contained in the other features. Features where the null hypothesis is rejected are labeled as discoveries (i.e., potential drivers of the observed response). Controlling the rate of false discoveries is crucial to ensuring analysis results are reliable. Yet in many scientific studies, feature selection is performed heuristically, without any statistical guarantees or control over the error rate.

This paper introduces the holdout randomization test (HRT) as a new approach to feature selection. At a high level, the HRT works by repeatedly evaluating a predictive model π on test data. The prediction quality of $\pi(X)$ is compared to $\pi(\tilde{X})$, where \tilde{X} is a copy of X that replaces the feature $X_{\cdot j}$ to be tested with a null sample $\tilde{X}_{\cdot j}$. This null sample is drawn from the *complete conditional* $P(X_{\cdot j}|X_{\cdot,-j})$, the distribution of the j^{th} feature given all other features. The complete conditional serves as a valid null model for Eq. (1) by preserving the joint dependency structure of $P(X)$ and removing any dependency between $X_{\cdot j}$ and Y . Intuitively, if $X_{\cdot j}$ actually has predictive power for Y then replacing it with a null sample $\tilde{X}_{\cdot j}$ is likely to lead to worse predictions. A p -value for the hypothesis test is then approximated by repeatedly resampling $\tilde{X}_{\cdot j}$ and comparing predictive performance under the null with performance using the original data.

The HRT works with any choice of predictor π and returns a valid p -value for each feature. The scientist does not need to consider the HRT when designing the predictive model, and the HRT does not need any knowledge of the model internals. The scientist is responsible only for constructing a strong predictor, with the understanding that a better model will typically lead to more discoveries. The HRT only needs to be able to query the model for predictions in order to perform feature selection. This decoupling enables the scientist to easily add the HRT to their analysis pipeline, making it a drop-in replacement for heuristic feature selection procedures.

The majority of the paper is dedicated to three aspects of the HRT:

Power Any predictive model can be used with the HRT, but its power increases with the quality of the predictor. Scientists can therefore focus on building the best predictive model they can. A better predictor will tend to yield more discoveries.

Robustness In practice, the conditional null distribution is unknown and must be estimated from data. The HRT is theoretically robust to estimation errors. Empirically, it produces conservative p -values when the null distribution is poorly estimated.

Computational efficiency The HRT is tailored to machine learning models where prediction is faster than model fitting. By only relying on test error, the HRT is computationally less expensive than feature selection methods that rely on model refitting.

1.1 Connections to existing work

Most classical work on feature selection relies on strong parametric assumptions. However, a flurry of recent techniques have been proposed to extract information from black box models. We contextualize the HRT in relation to these methods.

Many approaches are model-specific. Examples include iterative random forests (Basu et al., 2018), Bayesian kernel regression (Crawford et al., 2018), and Bayesian neural networks (Liang et al., 2018). These approaches constrain the scientist to a specific modeling

choice, rather than allowing the scientist to choose the best model or build a custom one specific for their problem. An advantage of the HRT is that it maximizes the freedom of the scientist to build the best predictive model they can, with reassurance that strong-performing models are likely to have high power.

Other methods focus on interpretation of the model, rather than testing for conditional independence. These include LIME (Ribeiro et al., 2016), DeepLIFT (Shrikumar et al., 2017), SHAP (Lundberg and Lee, 2017), and L2X (Chen et al., 2018). The latter two methods, SHAP and L2X, are related to the HRT in that they measure the conditional mutual information between each feature and the response. This can be seen as an optimization variant of the HRT where the statistic is change in prediction rather than prediction accuracy; however, for computational purposes both methods make simplifying independence assumptions between covariates that may lead to false positives. Even with a correct model for measuring mutual information, interpretability of the model is a related, but subtly different question. A poor model may use some true-null feature to make its predictions, in which case a correct interpretation would be to flag that variable as important to the model’s prediction, even though it is independent of the true label. An incorrect model is not a problem for the HRT; it will simply have low power to detect the true signals. See (Fisher et al., 2018) for an in-depth discussion on different notions of variable importance.

We are aware of only four methods for feature selection in arbitrary black box models. We describe and compare the HRT against each method in detail below.

Conditional randomization tests (CRTs) Candes et al. (2018) proposed CRTs as a generic approach for performing the conditional independence test in Eq. (1) using any test statistic and any predictive model. A CRT repeatedly samples from the conditional null for the feature being tested and compares the test statistic under the null with the test statistic of the original data. Unfortunately, this generality comes at a computational cost: refitting the model. For instance, the example test statistic considered by the authors was the feature coefficient magnitude in a lasso regression. In order to calculate the test statistic under a null sample, the regression must be re-run using the null data. Repeating this many times to approximate the feature p -value is prohibitively expensive computationally. The basic HRT is a special case of the CRT, where the test statistic is carefully chosen to avoid the need to refit after every null sample. Additionally, the theoretical analysis in Section 3 and practical improvements to the robustness and efficiency of the HRT in Section 4 are directly applicable to any CRT.

Model-X knockoffs Although Candes et al. (2018) originally proposed the CRT procedure, they discarded it in favor of the *model-X knockoffs* approach for the computational purposes outlined above. In the model-X knockoffs framework, a “knockoff” feature is generated for every feature in the dataset and the model is fit using both the original and knockoff features. Generating the knockoffs requires knowing (or estimating) the joint distribution over the features; selection is performed by a model-specific variable importance function for the original and knockoff features. Knockoffs have received a lot of attention in the literature, such as extensions to different feature distributions than the original multivariate normal (e.g. hidden Markov models (Sesia et al., 2017), Gaussian mixture models (Gimenez et al., 2018)). Others have suggested altering certain black box models to support knockoffs, such as using a special input layer in neural networks (Lu et al., 2018). While knockoffs have an appealing computational efficiency, they also contain several drawbacks that hinder their

adoption in scientific pipelines: i) a valid model of the joint distribution of the covariates must be obtainable, though recent work (Barber et al., 2018) shows knockoffs have similar robustness properties to CRTs; ii) a knockoff statistic must be chosen, which is model-specific and requires knowing something about the model internals; and iii) they require advanced thought and design from the scientist. This last point is worth stressing.

The scientist must decide before any predictive modeling is done that feature selection will be carried out via knockoffs. The knockoff variables must be included in the covariate set and screened similarly to the real covariates, which complicates leveraging external data sources (e.g. gene regulatory pathway information in predicting drug response from expression data). Even if knockoffs can be incorporated, it is unclear whether doubling the covariates will have an impact on the performance of the trained model, presenting a possible trade-off between predictive performance and feature selection power. Finally, if the scientist wishes to use the trained model to make any prediction on new data, corresponding knockoff samples must be generated for every prediction, which makes model usage awkward. The HRT, by contrast, enables the scientist to build a model that maximizes predictive performance without considering feature selection. Section 5.2 compares the HRT to knockoffs and shows that for the same lasso model the HRT has $\approx 3x$ higher power in simulation.

Mimic and Classify Sen et al. (2018) propose an approach inspired by generative adversarial networks (Goodfellow et al., 2014). Mimic and Classify fits a conditional model of the feature, similarly to a CRT, but then also fits a “discriminator” model to distinguish between samples from the true dataset and samples from the null model, with the difference in error magnitude as the test statistic. This is conceptually similar to the HRT but differs in key ways: i) it does not leverage a pre-built predictive model at all, ii) it does not provide direct p -value calculation, iii) it requires fitting a discriminator per hypothesis test, each of which may be as difficult to build as a predictive model for the response, and iv) it implicitly ties the magnitude of the dependency between X and Y to the test statistic, whereas the HRT is able to detect small but consistent performance differences between the original data and the null samples.

Conditional permutation tests (CPTs) Berrett et al. (2018) propose the CPT as a nonparametric alternative to the CRT. As in a classical permutation test, each feature’s support in a CPT is assumed to only be defined over the observed marginal distribution, but rather than randomly shuffling the feature, it is shuffled in a biased way similar to a CRT. CPTs are an interesting approach and are likely complementary to the HRT. In particular, they are more robust than CRTs in practice and may increase the robustness of the HRT even further. As with generic CRTs, the robustness and efficiency improvements in Section 4 also extend to CPTs.

2 The Holdout Randomization Test

2.1 Setup and notation

Throughout the paper, upper case symbols denote (e.g. X) matrix variables; the first subscript indexes the row (X_i) and the second indexes columns ($X_{\cdot j}$); negation indicates every element except the one(s) specified ($X_{\cdot, -j}$). Let $P_{j|-j} = \mathbb{P}(X_{\cdot j} | X_{\cdot, -j})$ denote the complete conditional of the j^{th} feature.

Consider the following predictive modeling scenario:

- We receive a dataset $\mathcal{D}^* = \{(X_i, Y_i)\}_{i=1}^{n^*}$ of n^* samples where $(X_i, Y_i) \stackrel{\text{iid}}{\sim} P$.
- The scientist specifies a predictive model class $\pi_\theta(X) \rightarrow \hat{Y}$ with parameters θ .
- Data is split into train and test sets, \mathcal{D} and \mathcal{D}' of n and n' samples, respectively.
- \mathcal{D} is used to fit $\hat{\theta}$ by optimizing an objective function $\mathcal{L}_\pi(\mathcal{D}, \theta)$.
- \mathcal{D}' is held out for evaluating the empirical risk $\mathcal{G}(\mathcal{D}', \pi_{\hat{\theta}}) = \frac{1}{n'} \sum_{i=1}^{n'} g(X_i, Y_i, \pi_{\hat{\theta}}(X_i))$.
- The inferential goal is to use $\pi_{\hat{\theta}}$ to conduct a conditional independence test for feature $X_{:,j}$ as in Eq. (1).

Fitting a single model may take hours or even days for large datasets and complicated models. Evaluating the model on the test set, however, is much faster and it is computationally feasible to perform many evaluations. We assume the scientist chooses their predictive model without looking at the test set.

2.2 Basic Method

The HRT procedure is presented in Algorithm 1. The HRT algorithm first fits the predictive model using the training dataset and the fitting procedure supplied by the scientist (Line 2). The fitting procedure and model choice are arbitrary. For instance, the scientist is free to use cross-validation of the training set to select model hyperparameters, bootstrap and aggregate multiple model fits, or add sparsity-inducing regularizers. Moreover, the scientist is encouraged to build the best predictive model they can. As we show in Section 5.3, there is a strong correlation between model quality and the power of the HRT when using the model.

Once fit, Algorithm 1 evaluates the empirical risk of the model (Line 3). This establishes a baseline for model performance on the original data. The HRT algorithm then repeatedly resamples $X_{:,j}$, the feature being tested, from the null distribution $P_{j|-j}$ (Line 5). This sampling procedure breaks any possible dependence between X_j and Y , but preserves the joint distribution structure of $P(X)$. Consequently, the samples are valid draws from null distribution where $X_{:,j}$ has no predictive power. For each null sample, the algorithm replaces the real feature values with the sampled null values (Line 6) and evaluates the empirical risk of the model on the new dataset (Line 7).

Empirical risk functions as a test statistic in the HRT. Algorithm 1 compares the risk (t) on the original data with risk (\tilde{t}) under the null. It then uses the null samples estimate the likelihood of observing an empirical risk as low as t , if H_0 were true. Adding 1 to the numerator and denominator in the average (Line 8) corrects for finite sampling; the result is a valid one-sided p -value for testing the null hypothesis in Eq. (1).

The validity of the p -value derives from the fact that it is a specialized version of a conditional randomization test (Candes et al., 2018). In CRTs, *any* test statistic and predictive model represent a valid conditional independence test. The key separator between the HRT and generic CRTs is in the construction of the test statistic. In the original construction, the test statistic is assumed to be a function of the entire dataset \mathcal{D}^* and the parameters $\hat{\theta}$ after fitting to the dataset. Evaluating a null sample then requires refitting the model to obtain a sample from the null distribution over θ . This makes CRTs prohibitively

Algorithm 1 Holdout Randomization Test

- 1: **procedure** HRT(training data \mathcal{D} , test data \mathcal{D}' , model π , training objective \mathcal{L}_π , empirical risk function \mathcal{G} , sample size K)
- 2: Fit $\hat{\theta}$ by optimizing $\mathcal{L}_\pi(\mathcal{D}, \theta)$.
- 3: Compute the empirical risk on held out data, $t \leftarrow \mathcal{G}(\mathcal{D}', \pi_{\hat{\theta}})$.
- 4: **for** $k \leftarrow 1, \dots, K$ **do**
- 5: Sample $\tilde{X}'_{\cdot j} \sim P_{j|\cdot j}$.
- 6: Create a new dataset $\tilde{\mathcal{D}}$ by replacing $X'_{\cdot j}$ in \mathcal{D}' with $\tilde{X}'_{\cdot j}$.
- 7: Compute the empirical risk, $\tilde{t}^{(k)} \leftarrow \mathcal{G}(\tilde{\mathcal{D}}, \pi_{\hat{\theta}})$.
- 8: **return** A (one-sided) p -value,

$$\hat{p}_j = \frac{1}{K+1} \left(1 + \sum_{k=1}^K \mathbb{I} \left[t \geq \tilde{t}^{(k)} \right] \right)$$

expensive to compute in practice. By defining the test statistic to focus only on predictive performance of a *fixed* model, the HRT requires no refitting at all. Only model evaluation is necessary, which is cheap enough in many machine learning models to make the HRT feasible for a large class of predictive models.

Strictly speaking, the train-test split is also unnecessary for the HRT. The motivation for its use is power. A valid test would be to fit a model on the entire dataset, fix the model, then run Algorithm 1 using a test statistic based on training set performance. For models that have successfully optimized their objective function, almost any change in coefficients will result in worse performance. Thus, every feature will fail to be rejected without any data partitioning.

Algorithm 1 focuses on simple scalar regression. In general, the HRT is valid for a much broader class of methods—effectively any predictive modeling scenario where empirical risk is measureable. In fact, the model fit need not even be very good and can be chosen by an adversary in the worst case. Similar to the unsplit dataset approach, poorly chosen models will also yield a model with zero power, but type I error will still be conserved.

The remainder of the paper addresses several pragmatic questions regarding the HRT:

- If we estimate the conditional $P_{j|\cdot j}$ from data, will the HRT be robust to small estimation errors? (Section 3)
- When the data is too small to ensure small estimation errors, can we somehow err on the side of caution and produce conservative p -values? (Section 4.1)
- Is it possible to use the entire dataset, rather than splitting it into train and test, so as to maximize power? (Section 4.2)
- Can we speed up the algorithm further? (Section 4.3)

3 Robustness of Conditional Randomization Tests

CRT procedures—such as the HRT—provide valid p -values under the assumption that we have access to the true complete conditional distributions $P_{j|\cdot j} = \mathbb{P}(X_j|X_{-j})$. This

assumption is not realistic. In practice, these distributions must be estimated from data. Here we show that CRT procedures are robust to misspecification of the conditional distribution subject to mild conditions.

Let $X \in \mathbb{R}^{N \times P}$ be a matrix of covariates and let $t(Y, X_j, X_{-j})$ be a test statistic for feature X_j where lower values of t represent a stronger degree of importance. For HRTs the statistic is the empirical risk on test data. The CRT p -value for the j^{th} covariate is:

$$\hat{p}_j^{\text{crt}} = \mathbb{E}_{\tilde{X}_j \sim P_{j|-j}} [\mathbb{1}\{t(Y, X_j, X_{-j}) \leq t(Y, \tilde{X}_j, X_{-j})\}]. \quad (2)$$

In practice, we approximate $P_{j|-j}$ by some other distribution $Q_{j|-j}$, typically learned from the data. The practical estimator is:

$$\hat{p}_j = \frac{1}{M} \sum_{k=1}^M \mathbb{1}\{t(Y, X_j, X_{-j}) \leq t(Y, \tilde{X}_j^{(k)}, X_{-j})\} \quad \tilde{X}_j^{(k)} \sim Q_{j|-j}. \quad (3)$$

For notational brevity, we denote the event $\{t(Y, X_j, X_{-j}) \leq t(Y, \tilde{X}_j, X_{-j})\}$ by $T_j(\tilde{X}_j)$, leaving the dependence on X, Y implicit (as with \hat{p}_j^{crt}). We will require the approximating distribution to satisfy the following conditions,

1. Pessimism bias:

$$\hat{p}_j^{\text{crt}} - \mathbb{E}_{Q_{j|-j}} [\mathbb{1}\{T_j(\tilde{X}_j)\}] \leq \epsilon$$

Intuitively, $\mathbb{E}_{Q_{j|-j}} [\mathbb{1}\{T_j(\tilde{X}_j)\}]$ is the estimated p -value (i.e., $M \rightarrow \infty$). For this to be conservative, it should be at least as large as \hat{p}_j^{crt} . We assume that we violate this condition by at most ϵ .

2. Subgaussianity. Let $Z = \mathbb{1}\{T_j(\tilde{X}_j)\} \frac{P_{j|-j}(\tilde{X}_j)}{Q_{j|-j}(\tilde{X}_j)} - \hat{p}_j^{\text{crt}}$. We assume Z is subgaussian. That is, there exists some constant σ such that:

$$\mathbb{E}_{Q_{j|-j}} [\exp(\lambda Z)] \leq \exp(\lambda^2 \sigma^2 / 2) \quad \forall \lambda \in \mathbb{R}.$$

Intuitively, we require some control over the quality of the approximation in the tails. Subgaussianity is a standard assumption of this kind. We make a slight modification by requiring a good approximation only in regions of the sample space where $T_j(\tilde{X}_j)$ occurs. That is, we allow poor approximation if it induces a bias towards higher p -values.

Theorem 1. *If both assumptions hold then*

$$\mathbb{P}(\hat{p}_j^{\text{crt}} - \hat{p}_j > 2\epsilon \mid X, Y) < 2 \exp\left(-M \frac{\epsilon^2}{2(1 + \sigma^2)}\right)$$

Proof. Let

$$\tilde{p}_j = \frac{1}{M} \sum_{k=1}^M \mathbb{1}\{T_j(\tilde{X}_j^{(k)})\} \frac{P_{j|-j}(\tilde{X}_j^{(k)})}{Q_{j|-j}(\tilde{X}_j^{(k)})}$$

be an importance reweighted estimate for \hat{p}_j^{crt} . We will bound $\hat{p}_j - \tilde{p}_j$ and $\tilde{p}_j - \hat{p}_j^{\text{crt}}$.

Note that

$$\hat{p}_j - \tilde{p}_j = \frac{1}{M} \sum_{k=1}^M \mathbb{1}\{T_j(\tilde{X}_j^{(k)})\} \left(1 - \frac{P_{j|-j}(\tilde{X}_j^{(k)})}{Q_{j|-j}(\tilde{X}_j^{(k)})}\right)$$

By pessimism bias,

$$\mathbb{E}_{Q_{j|-j}}[\mathbb{1}\{T_j(\tilde{X}_j^{(k)})\} \left(1 - \frac{P_{j|-j}(\tilde{X}_j^{(k)})}{Q_{j|-j}(\tilde{X}_j^{(k)})}\right)] = \mathbb{E}_{Q_{j|-j}}[\mathbb{1}\{T_j(\tilde{X}_j^{(k)})\}] - \hat{p}_j^{\text{crt}} \geq -\epsilon,$$

so that

$$\mathbb{P}(\hat{p}_j - \tilde{p}_j < -2\epsilon) \leq \mathbb{P}\left(\frac{1}{M} \sum_{k=1}^M \mathbb{1}\{T_j(\tilde{X}_j^{(k)})\} \left(1 - \frac{P_{j|-j}(\tilde{X}_j^{(k)})}{Q_{j|-j}(\tilde{X}_j^{(k)})}\right) - \mathbb{E}_{Q_{j|-j}}[\mathbb{1}\{T_j(\tilde{X}_j^{(k)})\} \left(1 - \frac{P_{j|-j}(\tilde{X}_j^{(k)})}{Q_{j|-j}(\tilde{X}_j^{(k)})}\right)] < -\epsilon\right).$$

By the subgaussianity assumption, the random variables

$$\mathbb{1}\{T_j(\tilde{X}_j^{(k)})\} \left(1 - \frac{P_{j|-j}(\tilde{X}_j^{(k)})}{Q_{j|-j}(\tilde{X}_j^{(k)})}\right) - \mathbb{E}_{Q_{j|-j}}[\mathbb{1}\{T_j(\tilde{X}_j^{(k)})\} \left(1 - \frac{P_{j|-j}(\tilde{X}_j^{(k)})}{Q_{j|-j}(\tilde{X}_j^{(k)})}\right)]$$

are subgaussian with subgaussian parameter $\sigma^2 + 1$, as can be checked directly from the definition of subgaussianity. Hoeffding's inequality for subgaussian random variables then immediately implies that

$$\mathbb{P}(\hat{p}_j - \tilde{p}_j < -2\epsilon) \leq \exp\left(-m \frac{\epsilon^2}{2(1 + \sigma^2)}\right). \quad (4)$$

Hoeffding's inequality for subgaussian random variables also yields that

$$\mathbb{P}(\tilde{p}_j - \hat{p}^{\text{crt}} < -\epsilon) \leq \exp\left(-m \frac{\epsilon^2}{2\sigma^2}\right). \quad (5)$$

The claim is immediate from Eq. (4) and Eq. (5). □

Barber et al. (2018) study the robustness of the knockoff procedure to misspecification of the knockoff sampling distribution. They show that the inflation of the false discovery rate is controlled by the discrepancy between the true complete conditionals and the complete conditional of the misspecified knockoff distribution. They use a strong notion of discrepancy closely related to KL divergence. Berrett et al. (2018) consider CRTs and show that the inflation of the false discovery rate is controlled by the total variation distance between $P_{j|-j}$ and $Q_{j|-j}$. Both papers establish converse results showing that it's possible to adversarially construct a testing procedure that has FDR inflation that grows with the (KL or total variation) discrepancy. The assumption we make on $Q_{j|-j}$ is weaker than either of the previously considered notions. This is possible because we first fix the test statistic and then ask for Q to be a good proxy with respect to that particular test. The previous results demand uniform control over all test statistics.

4 Modeling details: making the HRT more robust, powerful, and efficient

4.1 Conservative sample-reweighting for small-sample FDR control

In high-dimensional datasets, the error in the estimated $Q_{j|-j}$ will not satisfy the subgaussianity assumption of Section 3. This error can lead to inflated tails of the null p -values, causing a violation of the Type I or FDR error threshold. Here we develop a calibration technique that aims to produce conservative p -values by pessimistically weighting each null sample comparison.

We begin by casting Algorithm 1 as an importance sampling scheme with $Q_{j|-j}$ as a proposal distribution,

$$\hat{p}_j \approx \frac{1}{1 + \sum_{k=1}^K W^{(k)}} \left(1 + \sum_{k=1}^K \mathbb{1} \left\{ \mathcal{G}(\mathcal{D}', \pi_{\hat{\theta}}) \geq \mathcal{G}(\tilde{\mathcal{D}}^{(k)}, \pi_{\hat{\theta}}) \right\} W^{(k)} \right), \quad (6)$$

$$\tilde{\mathcal{D}}^{(k)} = [\tilde{X}_{\cdot j}^{(k)}, X'_{-j}], \quad \tilde{X}_{\cdot j}^{(k)} \sim Q_{j|-j},$$

where $W^{(k)}$ is the importance weight,

$$W^{(k)} = \frac{P_{j|-j}(\tilde{X}_{\cdot j}^{(k)})}{Q_{j|-j}(\tilde{X}_{\cdot j}^{(k)})} \quad (7)$$

The estimate in (6) is consistent, but it still relies on the unknown true conditional $P_{j|-j}$, making it impossible to compute in practice.

Let $f_{j|-j}$ and $h_{j|-j}$ be functions that bound the true probability of the null sample: $0 \leq f_{j|-j}(\tilde{X}_{\cdot j}) \leq P_{j|-j}(\tilde{X}_{\cdot j}) \leq h_{j|-j}(\tilde{X}_{\cdot j})$. If we have access to such a function, we can then bound p_j in expectation by biasing the importance weights to be conservative. This works by choosing the importance weight dynamically based on the outcome of each test statistic comparison,

$$\widehat{W}^{(k)} = \begin{cases} \frac{f_{j|-j}(\tilde{X}_{\cdot j}^{(k)})}{Q_{j|-j}(\tilde{X}_{\cdot j}^{(k)})} & \text{if } \mathcal{G}(\mathcal{D}', \pi_{\hat{\theta}}) < \mathcal{G}(\tilde{\mathcal{D}}^{(k)}, \pi_{\hat{\theta}}) \\ \frac{h_{j|-j}(\tilde{X}_{\cdot j}^{(k)})}{Q_{j|-j}(\tilde{X}_{\cdot j}^{(k)})} & \text{otherwise.} \end{cases} \quad (8)$$

Under this conservative weighting, $\mathbb{E}[\hat{p}_j] \leq p_j$. The tighter the bound from $(f_{j|-j}, h_{j|-j})$, the less conservative the p -value estimate and thus the more powerful the test statistic. Trivially, for any true $P_{j|-j}$, we can always choose $f_{j|-j} = 0$ and guarantee \hat{p} will be conservative. It will always be 1, however, so the method will be without power. To be effective, the bound must be relatively tight.

This importance sampling view may not seem immediately helpful. We appear to have simply traded off the requirement of having the true complete conditional distribution for a requirement of having bounds on that same distribution. Fortunately, it is straightforward to extend the proof from Section 3 to show that the weighting scheme is robust to errors in the bound. This means we only need good approximate bounds on $P_{j|-j}$, which is tractable with much fewer samples than the exact bounds or a good approximation of $P_{j|-j}$.

A natural way to generate approximate bounds on $P_{j|-j}$ is to use a conditional density estimation (CDE) method that quantifies uncertainty. Bounds can be obtained by picking

upper and lower quantiles such that the theoretical robustness properties apply. For instance, when using a Bayesian method, quantiles can be derived either analytically or approximately by sampling from the posterior via Markov chain Monte Carlo. Since we wish to remain maximally flexible to the form of $P_{j|-j}$, we treat the CDE model as a black box and use the bootstrap to generate quantiles (see Efron and Tibshirani, 1998, for a discussion on the technical issues with using the bootstrap for confidence intervals).

We create b bootstrap resamples of the dataset and fit b corresponding CDE models $B_{j|-j} = (Q_{j|-j}^{(1)}, Q_{j|-j}^{(2)}, \dots, Q_{j|-j}^{(b)})$, with $Q_{j|-j}^{(1)}$ used as the proposal distribution. Given a choice of lower and upper quantile, (l, u) , we can replace the reweighting scheme in (8) with an approximate one,

$$\widehat{W}^{(k)} = \begin{cases} \frac{B_{j|-j}^{(l)}(\tilde{X}_{\cdot j}^{(k)})}{Q_{j|-j}^{(1)}(\tilde{X}_{\cdot j}^{(k)})} & \text{if } \mathcal{G}(\mathcal{D}', \pi_{\hat{\theta}}) < \mathcal{G}(\tilde{\mathcal{D}}^{(k)}, \pi_{\hat{\theta}}) \\ \frac{B_{j|-j}^{(u)}(\tilde{X}_{\cdot j}^{(k)})}{Q_{j|-j}^{(1)}(\tilde{X}_{\cdot j}^{(k)})} & \text{otherwise.} \end{cases} \quad (9)$$

where $B_{j|-j}^{(i)}$ denotes the i^{th} quantile of the estimates in $B_{j|-j}$.

In practice, $X_{\cdot j}$ is a vector of conditionally-independent (given $X_{\cdot -j}$) variables and the conditional density estimates are made on a per-sample basis. We take the geometric mean of the ratio of constituent-to-proposal conditional probability estimate \mathbb{G} for each model across all n samples,

$$\widehat{W}^{(k)} = \begin{cases} \left(\prod_{i=1}^n \frac{B_{j|-j}^{(l)}(\tilde{X}_{ij}^{(k)})}{Q_{j|-j}^{(1)}(\tilde{X}_{ij}^{(k)})} \right)^{1/n} & \text{if } \mathcal{G}(\mathcal{D}', \pi_{\hat{\theta}}) < \mathcal{G}(\tilde{\mathcal{D}}^{(k)}, \pi_{\hat{\theta}}) \\ \left(\prod_{i=1}^n \frac{B_{j|-j}^{(u)}(\tilde{X}_{ij}^{(k)})}{Q_{j|-j}^{(1)}(\tilde{X}_{ij}^{(k)})} \right)^{1/n} & \text{otherwise.} \end{cases} \quad (10)$$

Bootstrapping solves the first half of the calibration dilemma by providing a model-agnostic, nonparametric way to generate arbitrary quantile estimates. The other requirement is a way to actually choose the upper and lower quantiles. For this, we leverage the IID property of the conditional CDF values for each sample.

If a sampling distribution $Q_{j|-j}$ is well-calibrated, the distribution of CDF values for all samples should be uniform. In practice, this does not happen when using highly-flexible black box conditional density estimators trained via maximum likelihood estimation. While many approaches to recalibration have been explored in the literature, most tend to apply to classification or regression models (e.g. Platt scaling (Platt et al., 1999)). It is not immediately clear how one can calibrate quantiles for black box conditional density estimates. We use a data-adaptive strategy described in Appendix A for continuous random variables; for other data types, we recommend simply using $(l, u) = (5, 95)$ as a conservative choice.

4.2 Higher power via a cross-validation extension

Modeling pipelines typically allocate the bulk of the total data to the training set, leaving only 10–20% for testing. Since the HRT only uses the test set and the trained model, the majority of the data will not be used for testing. In scientific settings where sample sizes are small-to-moderate, discarding this much data may result in the HRT having low power. Here

Algorithm 2 Cross-Validation Holdout Randomization Test

1: **procedure** CV-HRT(training data split into M folds: $\mathcal{D} = \{\mathcal{D}^{(1)}, \mathcal{D}^{(2)}, \dots, \mathcal{D}^{(M)}\}$,
model π , training objective \mathcal{L}_π , empirical risk function \mathcal{G} , sample size K)
2: Initialize $t \leftarrow 0$
3: **for** $m \leftarrow 1, \dots, M$ **do**
4: Fit $\hat{\theta}^{(m)}$ by optimizing $\mathcal{L}_\pi(\mathcal{D}^{(-m)}, \theta)$.
5: Add the fold empirical risk, $t \leftarrow t + (1/M)\mathcal{G}(\mathcal{D}^{(m)}, \pi_{\hat{\theta}^{(m)}})$.
6: **for** $k \leftarrow 1, \dots, K$ **do**
7: Sample $\tilde{X}'_{\cdot j} \sim P_{j|\cdot j}$.
8: Create a new dataset $\tilde{\mathcal{D}}$ by replacing $X'_{\cdot j}$ in \mathcal{D}' with $\tilde{X}'_{\cdot j}$.
9: Initialize $\tilde{t}^{(k)} \leftarrow 0$
10: **for** $m \leftarrow 1, \dots, M$ **do**
11: Add the fold generalization loss on the randomized data,
$$\tilde{t}^{(k)} \leftarrow \tilde{t}^{(k)} + (1/M)\mathcal{G}(\tilde{\mathcal{D}}^{(m)}, \pi_{\hat{\theta}^{(m)}}).$$

12: **return** A (one-sided) p -value,

$$\hat{p}_j = \frac{1}{K+1} \left(1 + \sum_{k=1}^K \mathbb{I} \left[t \geq \tilde{t}^{(k)} \right] \right)$$

we show how the train-test paradigm of the basic HRT can be extended to a cross-validation paradigm that uses the entire dataset.

The cross-validation holdout randomization test (CV-HRT) is presented in Algorithm 2. The CV-HRT splits the data into M folds, rather than the train-test split of the basic HRT. The algorithm fits M models, with the m^{th} model trained using the m^{th} fold as the holdout set. Predictions are made across the entire dataset, but only model m is used to make predictions for samples in the m^{th} fold. The test statistic is then the average empirical risk across all folds. In effect, the CV-HRT performs M basic HRTs. This leads to a higher-power, lower-variance estimate of the usefulness of the j^{th} feature in predicting Y .

The CV-HRT is an extension of the basic HRT procedure in Algorithm 1, and again inherits validity from being a CRT. Unlike the basic HRT, however, the CV-HRT takes full advantage of the dataset by building multiple models, with one valid test model per sample. This takes the CV-HRT closer to the original CRT procedure, which also uses the full dataset. The key difference is that CRTs as originally conceived would train a single model on the entire dataset, whereas the CV-HRT trains multiple models on subsets of the data. As with the basic HRT, this specialization enables the CV-HRT to avoid refitting the predictive models after every null sample.

Stronger predictive models in any HRT procedure are likely to capture more of the dependency structure between X and Y . Consequently, more folds leads to more training data per model, which in turn should lead to better predictive performance per model. In the extreme, leave-one-out cross-validation will maximize power, but this comes at the computational expense of fitting n models, which may be prohibitive. In practice, we observe much higher power from as few as 5 folds.

Algorithm 3 Fast Holdout Randomization Test

- 1: **procedure** FAST-HRT(training data \mathcal{D} , test data \mathcal{D}' , model π , training objective \mathcal{L}_π , empirical risk function \mathcal{G} , sample size K , grid size S)
- 2: Fit $\hat{\theta}$ by optimizing $\mathcal{L}_\pi(\mathcal{D}, \theta)$.
- 3: Compute the empirical risk on held out data, $t \leftarrow \mathcal{G}(\mathcal{D}', \pi_{\hat{\theta}})$.
- 4: Construct S -grid approximations, Z and $\tilde{P}_{j|-j}$ for $X'_{:j}$ and $P_{j|-j}$, respectively.
- 5: **for** $i \leftarrow 1, \dots, n'$ **do**
- 6: **for** $s \leftarrow 1, \dots, s$ **do**
- 7: Create a new sample (\tilde{X}_i, Y'_i) by replacing X'_{ij} in \mathcal{D}' with grid point Z_{is} .
- 8: Compute sample risk, $T_{is} \leftarrow g(\tilde{X}_i, Y'_i, \pi_{\hat{\theta}}(\tilde{X}_i))$.
- 9: **for** $k \leftarrow 1, \dots, K$ **do**
- 10: Sample grid points $\{z_i\}_{i=1}^{n'}$ proportional to their weight in $\tilde{P}_{j|-j}^{(i)}$.
- 11: Compute the empirical risk, $\tilde{t}^{(k)} \leftarrow \frac{1}{n'} \sum_{i=1}^{n'} T_{i, z_i}$.
- 12: **return** A (one-sided) p -value,

$$\hat{p}_j = \frac{1}{K+1} \left(1 + \sum_{k=1}^K \mathbb{I} \left[t \geq \tilde{t}^{(k)} \right] \right)$$

4.3 Faster p -value approximation by empirical risk decomposition

The HRT relies on random sampling to approximate the expectation of the indicator function in Algorithm 1. Unlike other randomization tests, however, the HRT assumes a fixed model and a test statistic that is a summation of independent components. These two properties can be leveraged to substantially speed up the computation of the p -value approximation.

Algorithm 3 presents the fast approximation algorithm. The Fast-HRT first creates finite grid approximations $\tilde{P}_{j|-j}$ to $P_{j|-j}$. It then queries the model at each point to create a matrix T of cached component risk scores. In the test statistic computation loop (Lines 9–11), the cached component scores are sampled proportional to their likelihood in the complete conditional. The Fast-HRT then averages these cached component scores rather than querying the predictive model. This lowers the computational complexity from $\mathcal{O}(Kn')$ to $\mathcal{O}(Sn')$. Empirically, when K is large (e.g. in the case of many candidate features being tested) the Fast-HRT is 1–2 orders of magnitude faster than the basic HRT.

The discretization step is unnecessary when dealing with discrete data. The Fast-HRT would still benefit computationally from the caching strategy, however. Similarly, if one were to use an HRT version of a conditional permutation test (Berrett et al., 2018), a similar caching strategy could be employed with a modification to the sampling strategy to ensure valid permutation draws.

4.4 Putting it all together: a fast, calibrated, cross-validation HRT

All three of the HRT enhancements above were described independently but are fully compatible with each other. Combining them together yields a faster, more powerful, robust HRT that takes between seconds and a few minutes to calculate a precise, conservative p -value on a laptop.

Fig. 1 shows a visual example of the combined algorithm. The calibration method from

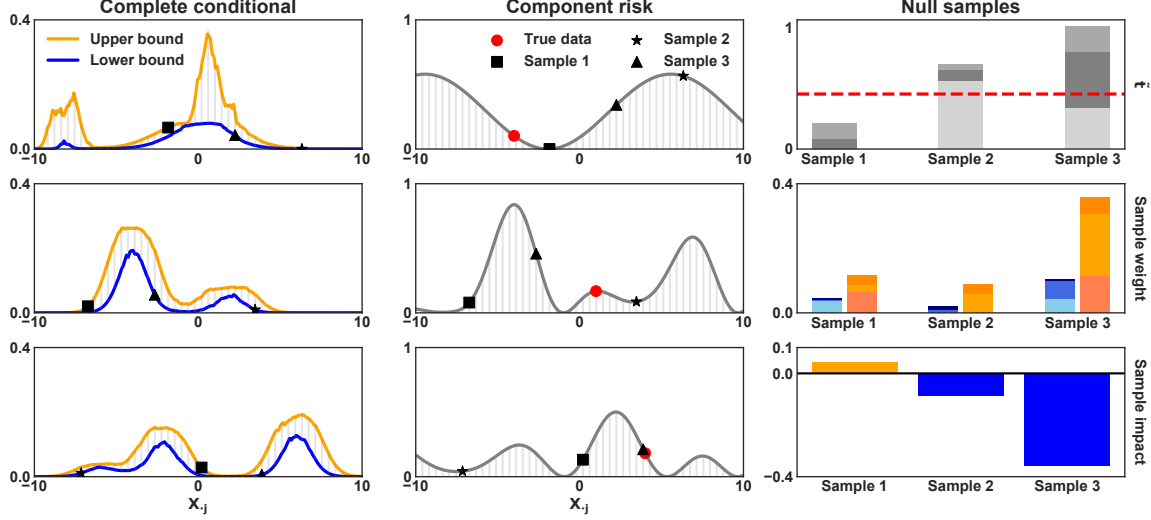


Figure 1: Visual depiction of the HRT with all enhancements described in Section 4, applied to a dataset of three samples with three null samples.

Section 4.1 returns bootstrapped upper and lower bound estimates for $P_{j|-j}$ in each sample (left column). The per-sample empirical risk for the model can be evaluated for any arbitrary value of the target feature (middle column). Gray bars in both the left and middle columns indicate the finite grid points used in the fast approximation; the bounds and empirical risk are evaluated at each grid point and cached. Null samples are then drawn from the grid approximation, proportional to the likelihood in the proposal distribution $Q_{j|-j}$.

The test statistic is calculated by summing over the cached component risk values for the sampled grid points (top right panel). Each null sample is associated with a likelihood weight corresponding to its lower (blue) or upper (orange) bounds for the sampled grid points (middle right panel). In the example, the first null sample has lower empirical risk than the original data (top right, dashed red line) and the other two null samples have higher empirical risk. Null samples where the empirical risk is below the threshold set by the original data are assigned the weight from the upper bound; other null samples are assigned the lower bound weight. Upper bound weights are added to the numerator and denominator in the final p -value calculation, causing the p -value to increase; lower bound weights are added only to the denominator, lowering the p -value estimation; we refer to this as the sample impact (bottom right panel).

5 Benchmarks

5.1 Setup

We benchmark the HRT on a variant of a benchmark from a recent paper on feature selection in Bayesian neural networks (Liang et al., 2018). We generate 100 independent datasets of 500 samples each with a nonlinear ground truth regression model,

$$y = \sum_{j=0}^9 [w_{4j}x_{4j} + w_{4j+1}x_{4j+1} + \tanh(w_{4j+2}x_{4j+2} + w_{4j+3}x_{4j+3})] + \sigma\epsilon, \quad (11)$$

where $\sigma = 0.5$ and $\epsilon \sim \mathcal{N}(0, 1)$. The 500 features are generated to have 0.5 correlation coefficient with each other,

$$x_j = (\rho + z_j)/2, \quad j = 1, \dots, 500, \quad (12)$$

where ρ and z_j are independently generated from $\mathcal{N}(0, 1)$.

The ground truth in (11) uses the first 40 features, representing true signals; each sample also contains 460 null features. We note that Liang et al. (2018) only had 4 signal features in their simulation. In preliminary simulations, the HRT had nearly 100% power and 0% FDR in this setting; we extend the experiment to 40 features to make the benchmark more challenging and model comparisons more informative.

We choose this setup for several reasons: (i) it is a nonlinear ground truth, (ii) most features are not involved in the response, (iii) all features are highly correlated, and (iv) it is compatible with the available implementation of model-X knockoffs (Candes et al., 2018) for the lasso; we compare to this implementation in Section 5.3.

For all experiments, we use a mixture density network (Bishop, 1994) with 5 components as the conditional density estimator in the HRT. For each feature, we fit a bag of $b = 100$ bootstrap estimators and use the data-adaptive calibration technique in Appendix A to choose the approximate lower and upper bounds. We use mean-squared error (MSE) as the empirical risk function. We select significant features with a target FDR of 10%, using the Benjamini-Hochberg procedure (Benjamini and Hochberg, 1995) for multiple testing correction.

5.2 Comparing the basic and enhanced HRT variants

We first compare several variants of the HRT procedure to investigate the effect of each component. For each dataset, the predictive model is a neural network with 2 hidden layers of 200 nodes each and ReLU activation functions; we fit the model using RMSprop with fixed learning rate 3×10^{-5} . We use an 80%/20% train/test split for the basic HRT and 5-fold cross-validation for the CV-HRT. Fig. 2 shows the power and FDR results for the different variants. We discuss the individual variants and results below.

Marginal Permutation. A common approach to testing for feature importance in many applications is the classical permutation test, where the values of a given feature are shuffled. Combining this with empirical risk on held out data was suggested by Breiman (2001) as a feature selection technique. To be valid, permutation testing requires that features are independent, which is explicitly not the case in the benchmark nor in many—if not most—real world datasets. The two left-most results in Fig. 2 show performance using a permutation approach, rather than the complete conditional, in both the basic and cross-validation HRT. The misspecified independence assumption causes an extreme inflation in the false discovery rate to nearly 80% instead of the target 10%.

Calibration. The middle two results in Fig. 2 show performance using a single, uncalibrated estimation of $P_{j|-j}$ in the basic and cross-validation HRT. The estimated conditional is a much better approximation of the true feature distribution than the marginal permutation above, but is still insufficient to control FDR at the target level. By contrast, the two right-most results show that the calibrated model better conserves FDR, with minimal impact on power compared to the uncalibrated model.

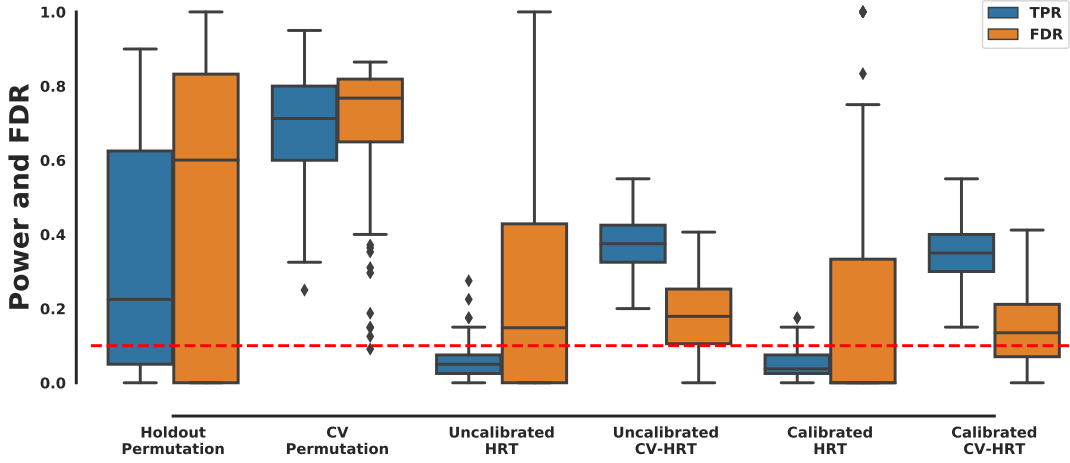


Figure 2: Power and FDR results for each HRT variant on the benchmark simulation. The calibration technique from Section 4.1 adjusts the sample weights to achieve tighter control over the FDR at the specified 10% level (dashed red line). Using cross-validation for predictive modeling increases power and reduces variance by using the entire dataset rather than just a held out subset.

Fig. 3 provides a closer look at the calibration procedure results for the cross-validation HRT. The top two panels show a sweep of possible choices of the upper and lower bounds for both power and FDR. Even at a stringent 90% confidence interval (top right corner of both heat maps), power is still 28%; FDR declines relatively rapidly, being only $\approx 5\%$ at a 90% interval. The bottom left panel shows the the CDF values of the p -values for the null features using different bounds. The panel is zoomed in to show the $[0, 0.1]$ region where p -values may be rejected under the target FDR threshold. Without any calibration, even the bootstrapped median (i.e. the $[50, 50]$ interval) still shows an inflation in the lower portion of the CDF, leading to invalid null p -values. A 20–30% confidence interval biases the null p -values down sufficiently to control the empirical FDR near the target level. The bottom right panel shows the distribution of bounds chosen by the data-adaptive procedure in each of the 100 independent trials; the procedure chooses roughly a 25% confidence region for most trials.

Basic HRT vs. CV-HRT. The right-most results in Fig. 2 demonstrate the effect of using a basic train-test split HRT versus a 5-fold cross-validation HRT. Cross-validation has the effect of boosting power and reducing variance compared to the basic HRT.

5.3 Model selection and knockoffs comparison

We next compare several choices of predictive model on the same benchmark task as above. Specifically, we ran the CV-HRT procedure with the neural network model from the previous section and the following alternative predictive models:

- Ordinary least squares (OLS)
- Partial least squares (PLS) with 10 components.
- Lasso with penalty parameter chosen via 5-fold cross-validation on each training set.

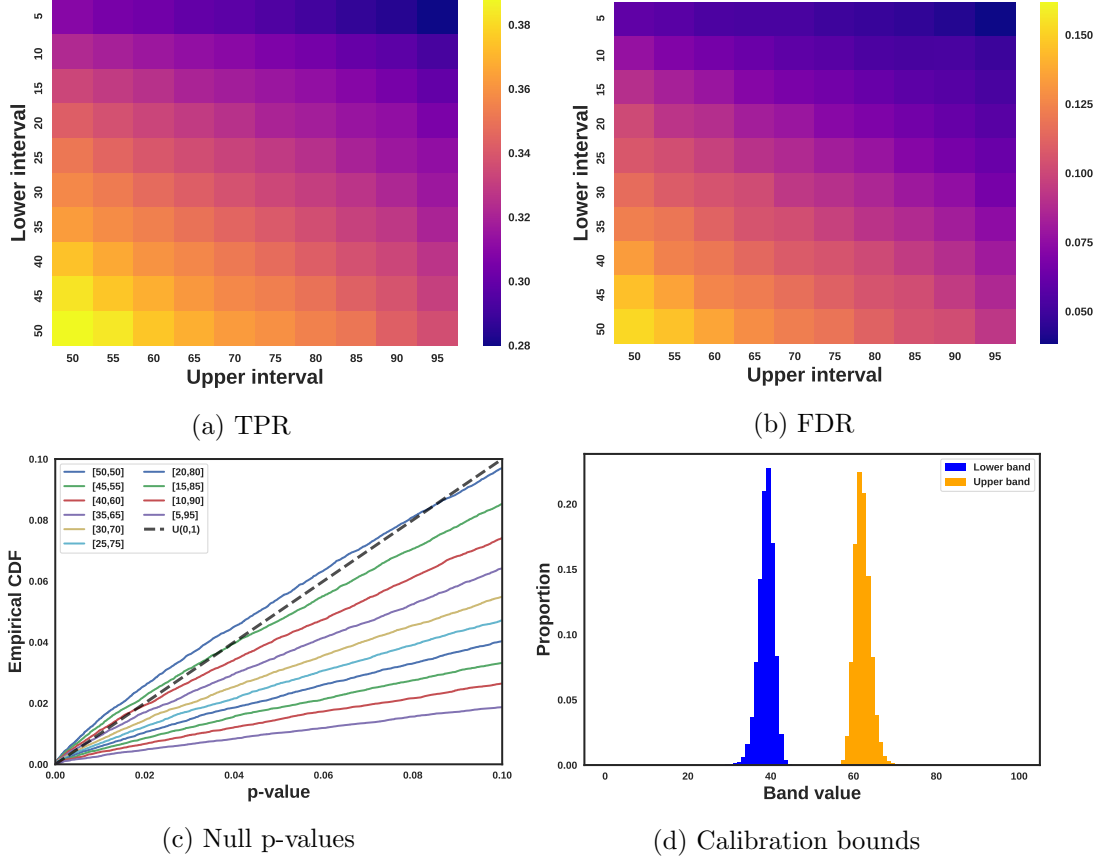


Figure 3: (a) TPR and (b) FDR for different fixed upper and lower quantile intervals on the benchmarks. (c) CDF of the true null p -values across all benchmark trials for different interval selections. (d) distribution of bounds selected by the calibration technique.

- Elastic net with both penalty parameters chosen via 5-fold cross-validation on each training set.
- Bayesian ridge with normal-inverse-gamma priors for coefficients and weakly informative scale hyperpriors.
- Kernel ridge with cubic polynomial kernel with a fixed penalty weight of 1.
- Support vector with radial basis function (RBF) kernel.
- Random forest with 20 trees.

All model hyperparameters not specified were set to their default in the `scikit-learn` Python package. We also compare to a lasso knockoff model using coefficient difference statistic; we use the implementation provided in the `knockoffs` R package.

Fig. 4 (top) shows the power and FDR results for each model. The predictive models are ordered by average cross-validation r^2 across all trials. CV-HRT power roughly increases with the quality of the predictive model, with the lasso model producing the highest power results. Fig. 4 (bottom right) demonstrates this with more granularity. It shows the power for each individual model on each trial as a function of the individual model r^2 . Even within

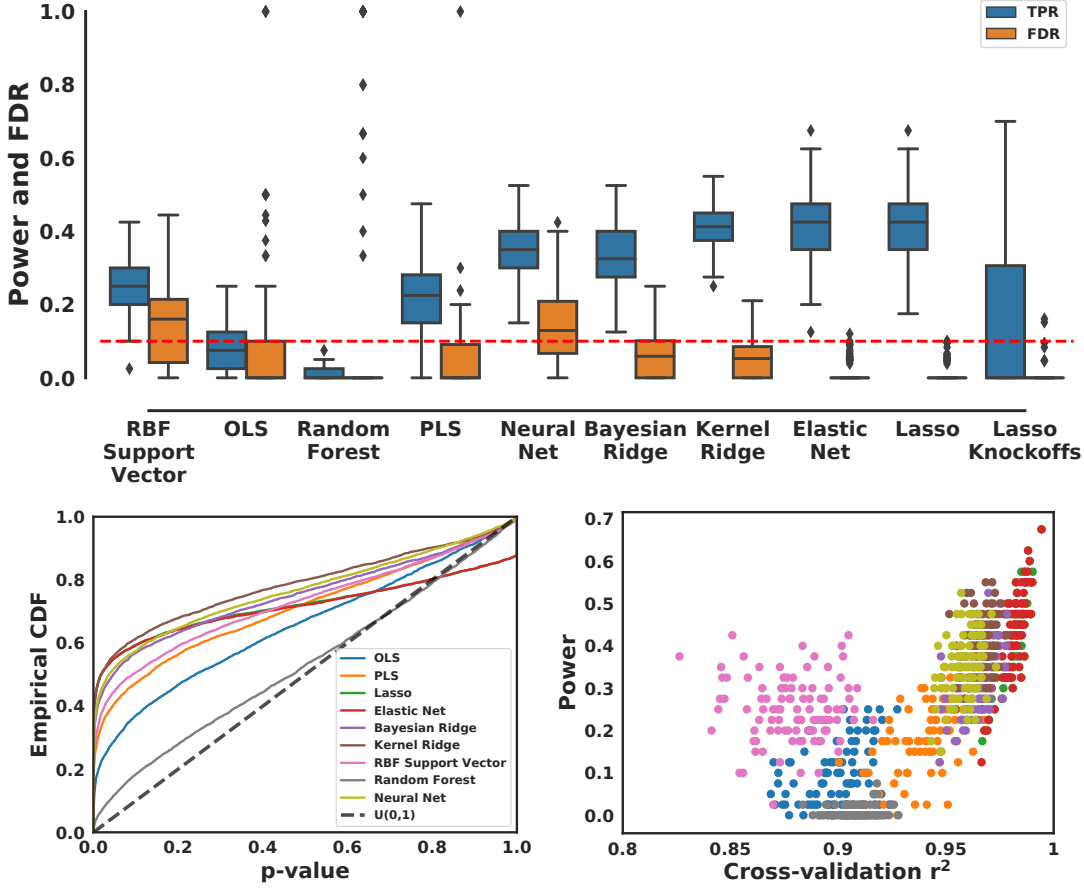


Figure 4: Top: Power and FDR for different choices of predictive model used in the CV-HRT, ordered by empirical risk of the predictive model. The right-most result is for a lasso model using model-X knockoffs for feature selection. Bottom left: distribution of p-values for signal features using each predictive model. Bottom right: predictive model performance versus feature selection power for each model and independent trial. Colors in the bottom right plot correspond to those in the bottom left.

the same model class, the models that generalize better tend to have higher power in the CV-HRT.

A notable exception is the random forest model, which has low power across all trials. This may be due to the nature of the model. Random forests average predictions from an ensemble of decision trees. Each tree predicts by recursively dividing into a series of half-planes, with each half-plane based on a single feature. Most null samples in the HRT are near, but slightly different than, the original data. It is likely that a small change to the original data will not change the random forest prediction, since it may not cause the feature to cross any half-plane. Since the comparison of the test statistic under the original model with each null sample statistic is not strict in the HRT, the insensitivity of random forests to small data changes leads to lower power. One solution to this is to use more trees in the forest, with data subsampling or bootstrapping to produce many different half-planes for each feature. Alternatively, switching to a conditional permutation HRT may boost power by generating more null samples where some feature values cross a hyperplane.

Fig. 4 also presents the results of a lasso knockoffs model. The power of the CV-HRT lasso model is approximately 3x more than knockoffs (45% versus 15% on average). This may be due to the difference in test statistics, with empirical risk being a more powerful statistic than coefficient magnitude. For instance, the equivalent lasso coefficient CRT proposed by Candès et al. (2018) had only 1.15x the power of knockoffs. However, knockoffs compare different subsets of the model parameters, not different instantiations of the data (as in the HRT). It is unclear how one could adapt knockoffs to work with empirical risk as a statistic.

6 Case studies from the scientific literature

6.1 Reporting features chosen by heuristics

We demonstrate the usefulness of the HRT on two datasets from real experiments. The first dataset measures the genomic profile of hundreds of cancer cell lines and their response to an anti-cancer drug. The second measures the molecular structure of hundreds of chemicals and their perceived olfactory properties. In both experiments, the original scientific analyses followed the same template: (i) a large number of features were gathered about the target, (ii) a predictive model was fit, (iii) a model-specific feature importance heuristic was used to rank features, and (iv) top-ranked features were reported as discoveries.

In both case studies, we followed the same procedures for steps (i) and (ii), but then replaced (iii) and (iv) with the calibrated CV-HRT. We use same conditional estimator as in Section 5, but for numerical stability take the first 100 principal components as inputs rather than raw features. We briefly describe each experiment and the original analysis approach, then present a comparison of the heuristics employed with the discoveries made by the HRT.

Drug response experiment The first dataset is a study of anti-cancer drug response in cancer cell lines (Barretina et al., 2012). Multiple drugs were tested against hundreds of cell lines; phenotypic response was measured as the area under the dose-response curve (AUC). Each cell line was analyzed to obtain gene mutation and expression features. The scientific goal is to discover the genomic features associated with drug response. Genomic features were first screened to filter out features with less than 0.1 magnitude Pearson correlation to the AUC. An elastic net model was fit for each drug, with hyperparameters chosen via 10-fold cross-validation. Features were then ranked by average coefficient magnitude. We choose a single drug, PLX4720, as an illustrative example. The results presented are similar to the original publication results for PLX4720, though not identical. We followed the analysis to the best of our ability, but the publicly available data is newer than the dataset used in the original publication. Our results are therefore different than those published, but not meaningfully so.

Olfactory perception experiment The second dataset is a study of the perceived fragrant properties of various molecules (Keller et al., 2017). Several hundred human subjects smelled and rated each molecule across 20 different categories. For each molecule, several thousand descriptive features about its chemical structure were measured. A random forest model was fit for each category to predict the average human rating given the features for a molecule. Different types of molecular descriptors were tried, with two sets (Dragon and Morgan descriptors) being selected based on performance on a held out test set. Features

(a) Elastic net for cancer drug response

Genomic Feature	Imp. score	Est. p -value
BRAF V600E Mut	0.0975	$\leq 10^{-5}$ *
RP11-208G20.3	0.0715	0.0065*
RP6-149D17.1	0.0665	0.2108
RNU6-104P	0.0652	0.9970
RNA5SP184	0.0634	0.3359
VPS13B Mut	0.0557	0.0042*
RP11-567M16.3	0.0535	0.0079*
MTMR11 Mut	0.0525	0.0821
ZNF549	0.0524	0.1915
HIP1 Mut	0.0519	$\leq 10^{-5}$ *

(b) Random forests for olfactory perception

Molecular Feature	Imp. score	Est. p -value
Isovanillin	0.2629	0.0012*
Vanillin isobutyrate	0.0528	0.2553
Ethyl vanillin	0.0481	0.0430
Ethyl vanillin acetate	0.0258	0.6066
Protocatechualdehyde	0.0236	0.1515
Vanillin acetate	0.0232	0.2845
2-Formylimidazole	0.0186	0.8132
R7e+	0.0179	0.5806
Ethyl Isovalerate	0.0123	0.7837
SM05 AEA(ri)	0.0099	0.2751

Table 1: Two examples of predictive modeling with heuristic post-hoc feature importance ranking in scientific studies. a) Genomic features were used to predict cell line response to treatment with the drug PLX-4720 (Barretina et al., 2012). b) Molecular features were used to predict perceived fragrant properties of molecules (Keller et al., 2017). Asterisks indicate features selected by the HRT at a 20% FDR threshold.

were then ranked by the random forest feature importance heuristic in `scikit-learn`. This heuristic estimates the expected number of samples in which a feature is used, based on how often and how deep it appears in the constituent trees. We again choose a single illustrative example, the *Bakery* category.

To increase power, we use the heuristics as a filter on which features to test in both case studies. Features with less than 10^{-3} heuristic importance (coefficient magnitude in elastic net and expected usage in random forests) are ignored. This leaves 873 features for the drug response dataset and 93 features for the olfactory perception dataset. This filtering step does not effect the statistical guarantees of the HRT since it is not based on any of the held out test data. It only avoids testing features that are completely ignored by the model and which the HRT will have no power to detect, if they are signals.

Table 1 shows the top 10 ranked features in both datasets, following their respective heuristics. Beside each feature, we report its heuristic importance score and the p -value assigned by the HRT. The heuristic rankings correlate poorly with the (theoretically grounded) p -value assigned by the HRT. Features with an asterisk denote those selected by the HRT with Benjamini-Hochberg correction at a 20% FDR threshold. It is impossible to know whether these features are all true positives, but the HRT demonstrates that the statistical evidence from the model does not match with the ranking heuristics.

6.2 Additional discoveries by the HRT

In the drug response experiment, the HRT selected additional features. Table 2 shows all discoveries by the HRT at a 20% FDR threshold that were not ranked in the top 10 by the heuristic. Alongside each feature we show its p -value estimate, heuristic score, and heuristic ranking. Several features were found to have significant predictive power despite their estimated model effect size being relatively low. This suggests there may be new potential targets of therapy worthy of follow-up investigation.

Genomic Feature	Heuristic ranking	Coefficient magnitude	Est. <i>p</i>-value
CNTN1 Mut	11	0.0512	0.0059
RNU6-448P	12	0.0486	0.0000
MIR4482-1	14	0.0474	0.0004
MTND4P25	19	0.0457	0.0010
RP11-585F1.8	20	0.0451	0.0058
RN7SL528P	21	0.0433	0.0034
KRTAP23-1	25	0.0384	0.0006
GS1-24F4.3	29	0.0372	0.0000
FLT3 Mut	31	0.0363	0.0000
RNU6-1287P	32	0.0360	0.0000
RP11-575H3.1	44	0.0294	0.0035
SNAPC3	51	0.0268	0.0012
RP11-541E12.1	55	0.0251	0.0000
RP11-488I4.2	70	0.0225	0.0012
RNA5SP234	72	0.0224	0.0000
CDC42BPA Mut	76	0.0213	0.0000
NEURL	79	0.0205	0.0000
RP11-481A12.2	82	0.0203	0.0002
HCP5	86	0.0200	0.0011
CTC-539A10.7	91	0.0190	0.0062
PIK3R4 Mut	98	0.0183	0.0025
SLC35G6	115	0.0165	0.0008
PIP5K1A Mut	122	0.0162	0.0002
CCND2 Mut	171	0.0123	0.0026
CDC37L1	178	0.0121	0.0000
CSPG4 Mut	211	0.0094	0.0003
RP5-1195D24.1	213	0.0094	0.0000
DIP2C Mut	256	0.0081	0.0003
RIOK3 Mut	358	0.0055	0.0049
POLR2J4	401	0.0047	0.0031
CACNA2D2	409	0.0046	0.0060
RNA5SP280	420	0.0044	0.0020
NTSR1 Mut	672	0.0018	0.0002

Table 2: Additional genomic features selected by the HRT at a 20% false discovery rate threshold in the drug response study, but not in the top 10 ranking of coefficient magnitude.

7 Discussion

When Leo Breiman wrote about the two cultures in statistics (Breiman, 2001), he divided statisticians into the *data modelers* and the *algorithmic modelers*. Data modelers relied on inflexible, idealized parametric models that make unrealistic assumptions about the true data generating distribution in order to gain the mathematical convenience of verification tools like goodness-of-fit tests. Algorithmic modelers chose to treat the latent function mapping features to response as a black box. In this latter paradigm, predictive performance on held out data was the only way to truly measure the strength of a model. Breiman estimated at the time that 98% of the mainstream analyst world fell into the data modeling crowd, while a mere 2% were algorithmic modelers.

Nearly 20 years later, the tables have turned. A confluence of factors (better numerical computing tools, the rise of Computer Science as one of the most popular majors in university, the dawn of the “Big Data” era, high throughput screening techniques in science, and the practical successes of machine learning) has led us to a world where algorithmic modeling is the norm and test error is the gold standard for model evaluation. The gravity of algorithmic modeling has grown so strong that it has even pulled in many scientific fields, leading to prediction challenges like the DREAM series (Stolovitzky et al., 2007). These challenges publicly release scientific data and teams compete to build the best model based solely on performance on held out test data. One would be hard pressed to argue that the algorithmic modelers are in the minority today.

Yet as we have shown, this shift has come at the cost of reliably extracting understanding from the data, what Breiman called the *information* goal. Articles in premier scientific journals now commonly use machine learning methods to build predictive models then derive scientific conclusions from ad-hoc model interpretation. These heuristic approaches rest on unstable ground that may lead scientists astray by convincing them a strong signal exists where there is none. Breiman himself nearly solved this by effectively proposing to use what we call the marginal permutation HRT (Section 5.2) as a means for interpreting random forests, but he failed to consider the need to account for feature dependency structure in his test. It is fitting then that rigorously extracting information from black box models, as the HRT does, requires using *more* black box modeling (i.e. conditional density estimators) to disentangle the features and perform a reliable conditional independence test.

There are several additional directions to explore for extending the HRT to other analysis settings. In some models, such as empirical Bayes models that use predictive models for prior estimation, inference is still too expensive to run the HRT. Efficiently searching over the space of potential features to test, using an approach like Bayesian optimization (Shahriari et al., 2016) or multi-armed bandit learning (Gandy and Hahn, 2017), would make applying the HRT to compute-intensive models feasible. In other scenarios, such as image classification, language modeling, and time series analysis, the features themselves have a more complicated structure and selecting an individual feature is not necessarily the inferential goal. For example, a pixel location being significant is not usually an interesting discovery in image classification. A conceptual layer needs to be added to extract meaningful insight in these types of models.

Finally, the HRT has the added benefit of allowing arbitrarily fine-grained questions to be asked. For instance, the scientist can partition the dataset based on some other feature, at which point the null hypothesis is $X_j \perp\!\!\!\perp Y | X_{\setminus k} = x, X_{\setminus (j,k)}$. This is a common test in biology, where predictive models are often trained on all of the data but questions are then asked about feature dependencies for specific samples, such as a specific type of cancer or

class of drug. We plan to explore these data-partitioning scenarios in future work.

References

- R. F. Barber, E. J. Candès, and R. J. Samworth. Robust inference with knockoffs. *arXiv preprint arXiv:1801.03896*, 2018.
- J. Barretina, G. Caponigro, N. Stransky, K. Venkatesan, A. A. Margolin, S. Kim, C. J. Wilson, J. Lehár, G. V. Kryukov, D. Sonkin, et al. The cancer cell line encyclopedia enables predictive modelling of anticancer drug sensitivity. *Nature*, 483(7391):603, 2012.
- S. Basu, K. Kumbier, J. B. Brown, and B. Yu. Iterative random forests to discover predictive and stable high-order interactions. *Proceedings of the National Academy of Sciences*, page 201711236, 2018.
- Y. Benjamini and Y. Hochberg. Controlling the false discovery rate: a practical and powerful approach to multiple testing. *Journal of the royal statistical society. Series B (Methodological)*, pages 289–300, 1995.
- T. B. Berrett, Y. Wang, R. F. Barber, and R. J. Samworth. The conditional permutation test. *arXiv preprint arXiv:1807.05405*, 2018.
- C. M. Bishop. Mixture density networks. Technical report, Citeseer, 1994.
- L. Breiman. Statistical modeling: The two cultures. *Statistical science*, 16(3):199–231, 2001.
- E. Candès, Y. Fan, L. Janson, and J. Lv. Panning for gold:model-xknockoffs for high dimensional controlled variable selection. *Journal of the Royal Statistical Society: Series B (Statistical Methodology)*, 2018.
- J. Chen, L. Song, M. J. Wainwright, and M. I. Jordan. Learning to explain: An information-theoretic perspective on model interpretation. *International Conference on Machine Learning*, 2018.
- L. Crawford, K. C. Wood, X. Zhou, and S. Mukherjee. Bayesian approximate kernel regression with variable selection. *Journal of the American Statistical Association*, pages 1–12, 2018.
- B. Efron and R. Tibshirani. The problem of regions. *The Annals of Statistics*, 26(5):1687–1718, 1998.

- A. Fisher, C. Rudin, and F. Dominici. Model class reliance: Variable importance measures for any machine learning model class, from the "rashomon" perspective. *arXiv preprint arXiv:1801.01489*, 2018.
- A. Gandy and G. Hahn. Quickmmctest: quick multiple monte carlo testing. *Statistics and Computing*, 27(3):823–832, 2017.
- J. R. Gimenez, A. Ghorbani, and J. Zou. Knockoffs for the mass: new feature importance statistics with false discovery guarantees. *arXiv preprint arXiv:1807.06214*, 2018.
- I. Goodfellow, J. Pouget-Abadie, M. Mirza, B. Xu, D. Warde-Farley, S. Ozair, A. Courville, and Y. Bengio. Generative adversarial nets. In *Advances in neural information processing systems*, pages 2672–2680, 2014.
- A. Keller, R. C. Gerkin, Y. Guan, A. Dhurandhar, G. Turu, B. Szalai, J. D. Mainland, Y. Ihara, C. W. Yu, R. Wolfinger, C. Vens, L. Schietgat, K. De Grave, R. Norel, , G. Stolovitzky, G. A. Cecchi, L. B. Vosshall, and P. Meyer. Predicting human olfactory perception from chemical features of odor molecules. *Science*, 2017. ISSN 0036-8075. doi: 10.1126/science.aal2014.
- F. Liang, Q. Li, and L. Zhou. Bayesian neural networks for selection of drug sensitive genes. *Journal of the American Statistical Association*, pages 1–18, 2018.
- Y. Y. Lu, J. Lv, Y. Fan, and W. S. Noble. Deeppink: reproducible feature selection in deep neural networks. *arXiv preprint arXiv:1809.01185*, 2018.
- S. M. Lundberg and S.-I. Lee. A unified approach to interpreting model predictions. In *Advances in Neural Information Processing Systems*, pages 4765–4774, 2017.
- J. Platt et al. Probabilistic outputs for support vector machines and comparisons to regularized likelihood methods. *Advances in large margin classifiers*, 10(3):61–74, 1999.
- M. T. Ribeiro, S. Singh, and C. Guestrin. Why should i trust you?: Explaining the predictions of any classifier. In *Proceedings of the 22nd ACM SIGKDD international conference on knowledge discovery and data mining*, pages 1135–1144. ACM, 2016.
- R. Sen, K. Shanmugam, H. Asnani, A. Rahimzamani, and S. Kannan. Mimic and classify: A meta-algorithm for conditional independence testing. *arXiv preprint arXiv:1806.09708*, 2018.
- M. Sesia, C. Sabatti, and E. J. Candès. Gene hunting with knockoffs for hidden markov models. *arXiv preprint arXiv:1706.04677*, 2017.

- B. Shahriari, K. Swersky, Z. Wang, R. P. Adams, and N. De Freitas. Taking the human out of the loop: A review of bayesian optimization. *Proceedings of the IEEE*, 104(1):148–175, 2016.
- A. Shrikumar, P. Greenside, and A. Kundaje. Learning important features through propagating activation differences. In *International Conference on Machine Learning*, pages 3145–3153, 2017.
- G. Stolovitzky, D. Monroe, and A. Califano. Dialogue on reverse-engineering assessment and methods. *Annals of the New York Academy of Sciences*, 1115(1):1–22, 2007.

A Approximate calibration via a one-way KS statistic

For continuous random variables, we propose a one-way Kolmogorov-Smirnov (KS) statistic to choose the lower and upper quantiles of the bootstrapped models. An adaptation to discrete random variables is also available in our implementation. For other types of features, we recommend a conservative bound of $(l, u) = (5, 95)$; we find this is sufficient to control FDR in preliminary experiments.

We describe the approach in terms of finding a lower bound; the upper bound is determined analogously. To choose a lower quantile, we start with the median ($l = 50$) and iteratively lower it until the CDF estimates dominate the uniform CDF from above in a Q-Q plot. Let $C_{j|-j}$ be the CDF for $B_{j|-j}$. The one-way lower-KS statistic for l is then,

$$\text{KS}^+(l) = \underset{c \in [0,1]}{\text{maximum}} \left(0, c - \frac{1}{n} \sum_{i=1}^n \mathbb{I} \left[C_{j|-j}^{(l)}(X_{ij}) \leq c \right] \right). \quad (13)$$

We then check if the current choice of l yields a sufficiently-small test statistic. Specifically, we conduct a hypothesis test by Monte Carlo, where we repeatedly draw samples from $U(0, 1)$ and only accept l if it is smaller than 10^5 draws from a true $U(0, 1)$. This corresponds to solving the following optimization problem:

$$\begin{aligned} \underset{l}{\text{argmax}} \quad & \max(0, \text{KS}^+(l)) \\ \text{subject to} \quad & \text{KS}^+(l) < \tau^+, \end{aligned} \quad (14)$$

where τ^+ is the MC-derived threshold; the upper quantile is found analogously. While the calibration procedure may seem very conservative, in practice it yields reasonable bounds even for the high-dimensional datasets in Section 5.